Effect of Cavity in Sandy Soil on Load Distribution of Pile Group

Dr. Mohammed Y. Fattah
Building and Construction Engineering Department, University of Technology, Baghdad.
Dr. Karim H. Ibrahim. Al-Helo
Building and Construction Engineering Department, University of Technology, Baghdad.
Hala H. Abed
Building and Construction Engineering Department, University of Technology, Baghdad.
Email: Halla.hani85@yahoo.com

Received on: 7/7/2013 & Accepted on: 6/3/2014

ABSTRACT

The present study investigates the influence of presence of cavities on adjacent buildings especially in the case of piled structures. The presence of cavity affects on the bearing capacity and settlement of piled foundation.

This paper presents an experimental study to investigate the behavior of model piles embedded in sandy soil of dry unit weight 16.8 kN/m^3. Model piles were tested in a sand box with load applied by a hydraulic compression jack and measured by means of a load cell. The settlement of the piles was measured by means of two dial gages; three strain gages were attached on piles to measure the strains and to calculate the load carried by each pile in the group by the strain indicator. Two types of piles (single pile and group of piles (1x2)) were tested in the laboratory as a free standing pile group.

A prototype of a cavity was used and placed adjacent to the piles at different distances from the pile centerline and different depths from the surface. The effect of variation of cavity locations (X), cavity depths (Y), and cavity diameter (d) on the load and settlement of the pile and groups of piles have been studied for all tests.

It was found that the presence of the cavity in the soil reduces the ultimate failure load of the pile. For single pile, the reduction rate is about (10% to 60%). For pile group (1x2), the reduction rate is about (40% to 80%). As intuitively expected, induced pile axial force is largest for the case where the level of the cavity is located below pile tip because the cavity is located within the zone of large displacement.

Keywords: Cavity, tunnel, Pile group, Sandy soil.

تأثير الفجوة في الترب الرملية على توزيع الحمل لمجموعة ركائز

الخلاصة

هذه الدراسة تبحث تأثير وجود الفجوات على المباني المجاورة خاصة في حالة المنشآت المستقرة على الركائز. إن وجود فجوة يؤثر على قابلية التحمل والهبوط للركيزة. يقدم هذا البحث دراسة تجريبية للتحقيق في تصرف نماذج ركائز مغروزة في تربة رملية ذات كثافة جافة تساوي (16.8 كيلونيوتن/م^3). تم إختبار نموذج ركائز في صندوق تربة يحتوي على رمل مع حمل مسلط باستخدام مكبس ضغط هيدروليكي ويقاس بما يسمى خلية الحمل. وقد تم قياس الإنفعالات على الركائز بأستخدام مقياس الإنفعال، حيث تم ربط ثلاثة مقاييس انفعال لكل ركيزة يتم من خلالها حساب الحمل الذي تحمله كل ركيزة في المجموعة بواسطة مؤشر الأنفعال. تم إختبار مجموعتين من الركائز (ركيزة واحدة و مجموعة ركائز (1×2)) مختبرياً بوصفها مجموعة ركائز حرة الإستناد.

إستخدم نموذج مصغر لفجوة وضعت بالقرب من الركائز تبعد عن مركز الركيزة بمسافات مختلفة وكذلك بأعماق مختلفة عن سطح التربة. وقد تم دراسة تأثير اختلاف مواقع الفجوة بالإتجاه الأفقي (X) والأعماق بالإتجاه العمودي (Y) وكذلك قطر الفجوة (d) على كل من الحمل والهبوط لركيزة ولمجموعة ركائز في جميع الإختبارات.

و قد وجود أن وجود الفجوة في التربة يقلل من التحمل الأقصى للركيزة. في الركيزة المفردة، يكون التقليل بالتحمل بحدود (10 – 60%) بينما في مجموعة الركائز (2 x 1) يكون التقليل بحدود (40 – 80%). و كما هو متوقع وجد أن الحمل المحوري على الركيزة أعلى ما يمكن عنما يكون مستوى الفجوة تحت مسنوى قاعدة الركيزة بسبب كون الفجوة واقعة ضمن المنطقة ذات الازاحة الكبيرة التي تسببها الركيزة.

INTRODUCTION

Cavities which occur under structures with sufficient frequency warrant special attention, since these cavities may cause structural damage and loss of lives. The precise investigations to locate the cavities and voids near the soil surface is one of the important factors where these cavities can be pose channels for the movement of water which expand and then collapse when they reach a critical size and therefore adversely affect the foundations of buildings, piles and other facilities.

These cavities exit in different structures which depend on the formation origin as follows (Aziz, 2008):

1) Artificial cavity due to the vault (oldest) building.
2) Natural cavity due to water flowing (the gypsum dissolution).

With continuous ground water movement in soils containing gypsum, the gypsum dissolves and generates many cavities of different shapes at various locations below ground surface. Different sizes of cavities are encountered in different sizes range between 10 cm to 300 cm (Aziz, 2008) as shown in Plate (1).

Plate (1): Photos of cavities with different sizes and locations (from Aziz, 2008).

Previous Studies

The influence of tunneling on adjacent buildings becomes an important problem. In urban areas, many high-rise buildings are supported by pile foundation and tunneling almost invariably will cause ground movements, which in turn will impose axial and lateral forces on the pile foundations.

Several researchers carried out a laboratory testing and centrifuge model testing respectively to investigate the effects of tunneling on the bearing capacity and deformation of the piles (Morton and King, 1979; Loganathan et al., 2000). They found that the influence of tunneling on adjacent piled foundation in weak soil may be of a great concern to geotechnical engineers.

Methods to analyze this problem may be classified broadly into two categories so far. The first of them is a complete three-dimensional analysis method which treats the piles and its surrounding soil as a whole during tunnel excavation, and usually 3D finite element method was used (Mroueh and Shahrour, 2002; Gordon and Ng, 2005; Lee and Jacobsz, 2006; Cheng et al., 2007).

The second class is so-called two-stage approach. First, free-field soil movements induced by tunneling are estimated by a simple analytical method, and, second, these estimated soil movements are then imposed on the pile in the analyses by using the finite element method, boundary element method or finite difference method of a beam to compute the pile responses (Chen et al., 1999; Loganathan et al., 2001; Xu and Poulos, 2001; Kitiyodom et al., 2005). Obviously, two-stage method is acceptable easily by engineering designers, especially which based on a simple Winkler model. However, there is currently almost no simple method available to analyze the influence of tunneling on piles considering shielding effect for passive pile groups.

The effects can be even more pronounced in the case of piled structures, as tunneling could potentially be carried out very close to piles. In addition, stresses

around piles are generally higher than near shallow foundations, so that stress relief associated with tunneling might have more pronounced effects.

Al-Taie (2004) studied the performance of laterally loaded piles embedded in sandy soils, which contain cavities. A program of laboratory testing was used in the study. The program of testing consisted of five groups: Group one was carried out on pile embedded in soil without cavities. The second and third groups were performed on pile embedded in soil containing single cavity located in front and in touch with pile face for the second group and in back and in touch with pile face for the third one. Group four was performed on pile with the existence of two cavities located in front and in touch with pile face. Group five was performed on pile with the existence of three cavities located in front and at a variable distance from pile face. All tests were performed on a free head pile subjected to horizontal load. The results indicated that the number of cavities and their location have a combined effect on the behavior of laterally loaded pile. The effect of cavities located in front of the pile is marginal at X/D > 8 where X is the spacing between cavity and pile and D is the diameter of the pile, see Figure (1).

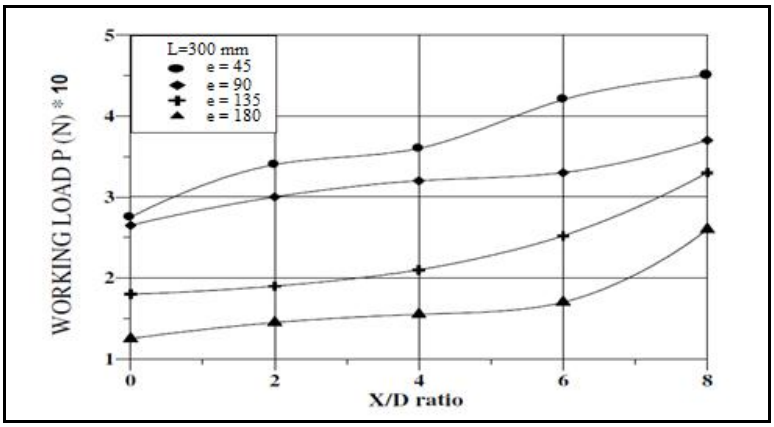

Figure (1): Variation of working load versus X/D at different load eccentricities (e) (group 5, three cavities, L= constant =300 mm) (after Al-Taie, 2004).

Cheng et al. (2004) investigated the influence of tunneling induced ground movements on existing piled foundations. Soil convergence around the tunnel excavation was modeled using a kinematic method. The results showed that for the case of a single floating pile, induced bending moments are generally negligible beyond a pile horizontal offset from tunnel centre (X) greater than 2 tunnel diameters (D_t) while pile cracking moment (Mcr) is easily exceeded with small tunnel volume loss for $X \leq 1D_t$. In addition, induced pile axial force is primarily dependant on i) position of pile tip relative to "zone of large displacements", ii) soil stiffness and iii) magnitude of volume loss. The zone of large displacements, zone of influence around the tunnel where piles might be affected, is generally enveloped by symmetrical boundaries extending upwards at an angle of 45° to the horizontal from the tunnel springline to the ground surface as shown in Figure (2).

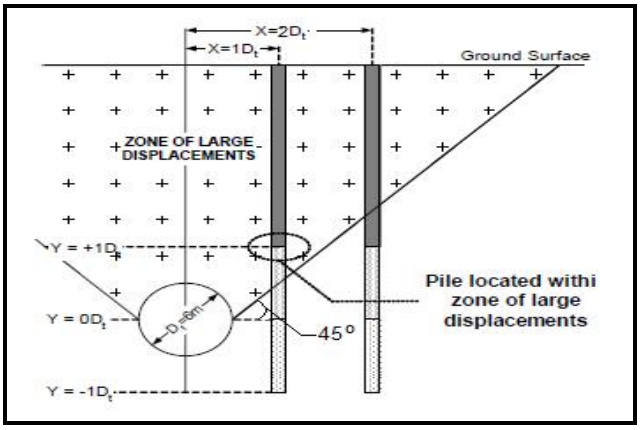

Figure (2): Location of pile tip relative to tunnel axis level and zone of large displacements (after Cheng et al., 2004).

Lee and Bassett (2007) investigated the influence zones for 2D pile–soil-tunneling interaction based on model test and numerical analysis. The study focused on two-dimensional laboratory model test for the pile–soil-tunneling interaction using a close range photogrammetric technique and numerical analysis. Schematic diagram for the model of the pile–soil-tunneling interaction test is shown in Figure (3). All piles were made of aluminum alloy with the same length (L = 370 mm), cross section (25 mm x 75 mm) and carried the same working load (P_w=27 kg). The model test results were found to be in good agreement with the finite element analysis. During the tunnel excavation, the pile unit showed a tendency for the tip to move towards the tunnel, resulting in a rotation off the vertical. In all model test series, the pile tip settlement showed a linear distribution within a volume loss V_L = 4%. The pile axial forces were greatly influenced by the location of pile tip from the tunnel centre line. The influence zones were dependent on the location of pile tip, 2D volume loss, soil strength, pile working load, pile size, dilation effect of the granular material, and tunnel size.

Experimental Work

Material used and soil properties

The sandy soil used in this study was obtained from one of construction sites in Erbil city. Standard tests were performed to determine the physical properties of the sand according to the **ASTM** specifications. The details of these properties are listed in Table (1).

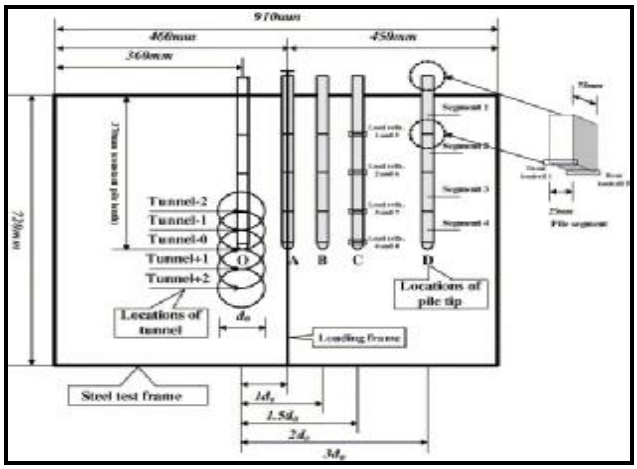

Figure (3): Schematic diagram for the pile–soil-tunneling interaction model test (after Lee and Bassett, 2007).

Table (1): Physical properties of the sand used in the tests.

Index property	Value	Specification
Specific gravity, G_s	2.63	ASTM D 854-2002
Effective size (mm), D_{10}	0.21	
Coefficient of uniformity, C_u	3.047	
Coefficient of curvature, C_c	0.911	
Soil classification (USCS)	SP	ASTM D 2487-2000
Maximum dry unit weight (kN/m^3), $\gamma_{d\,max}$	18.1	ASTM D 4253-2000
Minimum dry unit weight (kN/m^3), $\gamma_{d\,min}$	16.3	ASTM D 4254-2000
Dry unit weight (kN/m^3) at D_r=30%, γ_d	16.8	
Angle of internal friction at D_r=30%, ϕ	37º	ASTM D 3080-1998

USCS = Unified Soil Classification System.

The model of piles

The model of piles used in this study are smooth aluminum pipe piles. The external diameter of piles is (16 mm) with a wall thickness of (2 mm), while the length of piles is kept at (215 mm). The plate cap used for the model piles is also made of aluminum plate with a smooth surface having a thickness of (6 mm). A laboratory test was carried out to find the modulus of elasticity for an aluminum sample making use of the strain gage technique. A stress strain test was made in the laboratory to find the modulus of elasticity of the aluminum was found to be (65 GPa). The results are compatible with the finding of Al-Zayadi (2010).

Testing Setup

All model tests were conducted using the setup shown in Plate (2), which consists of frame, soil tank, and loading machine. The vertical load was applied to the model piles by means of 10 ton hydraulic compression handle jack. During all the experimental tests, the loading rate is kept approximately constant at (1 mm/min) for testing sandy soil as recommended by Bowels (1978). The applied load is measured using a "Sewha" load cell 5 ton capacity. A digital weighing indicator "Sewha" is used to read and display the load value. Two deformation dial gages with 0.01 mm sensitivity have been used for measuring displacements of the piled model.

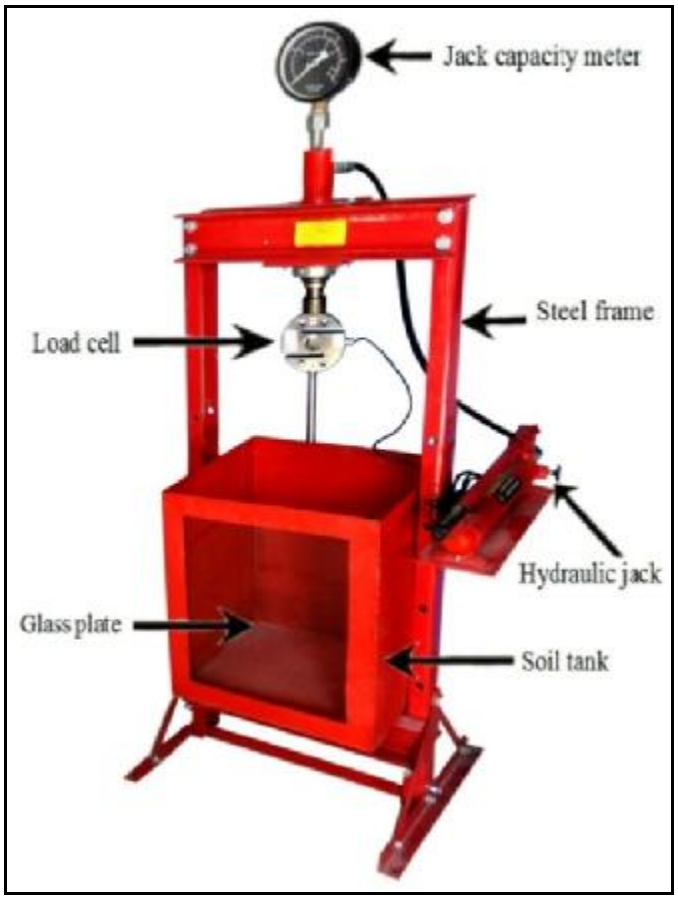

Plate (2): Testing setup.

Soil tank

The soil tank has (45 cm) length, (45 cm) width, and (50 cm) height. It was supported by the frame. The front side of the container consists of a glass plate (40 cm) in height, (35 cm) in width and (1 cm) in thickness. Through this glass, the position of the cavity can be seen in (X) and (Y) direction from the piles. The dimensions of the

tank were chosen so that the tank can be put inside the testing frame and there will be no interference between the walls of the soil tank and the failure zone around the piles.

Raining frame

A simple frame was used for controlling and obtaining the specific density using the sand raining technique. The frame consists of two columns connected together from one end and free from the other, the cone that is used to pour the sand was suspended at the connection end by means of cable through the pulley that was used to control the height of the cone.

Strain indicator

The Model P-3500 Strain Indicator is used to measure the strain in the piles as shown in Plate (3); the indicator belongs to in the Measurements Laboratory of the College of Engineering at Salahaddin University in Erbil.

Before adopting the results obtained from the strain indicator, external calibrations were made by testing a bar with known length by using the strain indicator and then by measuring the elongation using dial gages. The results of the two strain indicators were exactly the same.

Plate (3): Calibration of the strain indicator.

Strain gages

A strain gage, with gage factor equal to 2.0, was attached to the pile shaft and connected to a strain indicator to read the strain in the pile. Since the modulus of elasticity and the cross sectional area of the piles are known, then the amount of load carried by the pile can be obtained by using the following equation (Prakash, 1990):

$$Q_{av} = A\, E_p\, \varepsilon \qquad \ldots . (1)$$

where:

Q_{av} = load in the pile at the location of the strain gage,

A = cross section area of the pile,

ε = strain gauge reading, and
E_p = modulus of elasticity of the pile material.

Preparation of cavity model

Cavity model was made of circular aluminum pipes of very thin thickness approximately (1 mm) with a diameter of d = 16 mm. Cavity model was prepared by using a metal plate of aluminum (tin pack was used). After cutting the tin and making it as a plate, the plate was furl in diameter equal to the required diameter of the cavity (d) and in length equal to the length of the tank (45 cm).

Attachment of strain gages to the pile

Three strain gages 6 cm in length were placed along the pile shaft as shown in Plate (4). The readings of the three strain gages converged; the average of the three readings was used in the equation to obtain the load of the pile.

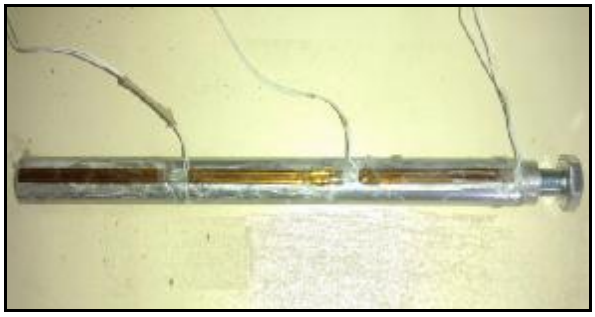

Plate (4): Attachment of strain gages to the pile.

Preparation of sand deposit and placing of piles and cavity

The bed of soil is prepared with a dry unit weight of (16.8 kN/m^3) at a height of drop equal to 80 cm. A rectangular steel mesh, specially made to help determine the position of the model pile groups, was placed on the top of the soil tank as shown in Plate (5). For the cavity, the placing is done during the process of sand raining at heights and distances computed according to research plan.

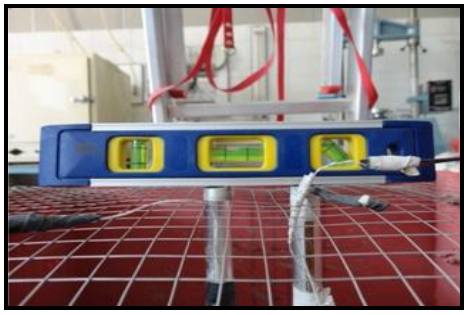

Plate (5): Placing of piles in the soil tank.

Testing program

Models of piles were used in the tests; the first model consists of 11 model single piles, while the second group consists of 12 model pile group (1x2). All these models have a similar geometry with regards to pile embedment length (L), pile diameter (D), and free length of the pile above the soil surface level equal to (1.5 cm) as shown in Figure (4).

The following variable parameters are studied in the tests, (see Figure 4):

1. Cavity location (X): the horizontal distance from centerline of the cavity to the centerline of the pile or group of piles, X=0 cm, 2.4 cm, 4.8 cm, and 8.8 cm.
2. Cavity depth (Y): the vertical distance from the soil surface to the cavity centerline, Y=10 cm, 20 cm, and 25 cm.

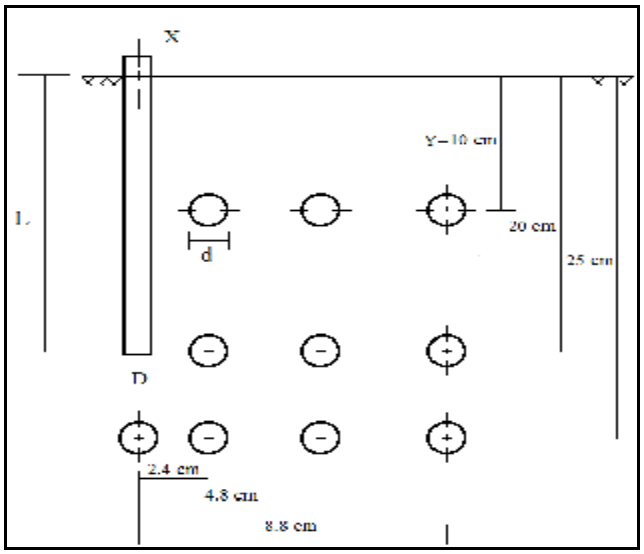

Figure (4): Problem geometry showing pile and cavity locations.

Analysis and Discussion of Test Results

To facilitate comparisons between the model tests, the geometric parameters are presented in terms of the following dimensionless forms:

(Y/L): the ratio of the depth of the cavity to the pile embedment length, Y/L=0.5, 1, and 1.25.

(X/D): the ratio of cavity location to pile diameter, X/D=1.5, 3, and 5.5.

(d/D): the ratio of cavity diameter to pile diameter, d/D=1.

For all model tests, the failure load adopted is that proposed by Terzaghi (1943) by which the failure load is defined as the load required to cause a settlement corresponding to 10% of pile diameter.

In this study, the results obtained from the laboratory tests have demonstrated the effect of cavity location, and cavity depth on the pile behavior in sandy soil.

Single pile

Figure (5) shows the load-settlement curve of a single pile embedded in a soil without cavity. Figure (6) shows the load-settlement curves of single pile embedded in soil with cavity of size ratio (d/D=1) located at different depths. The loads in these figures were measured by the load cell.

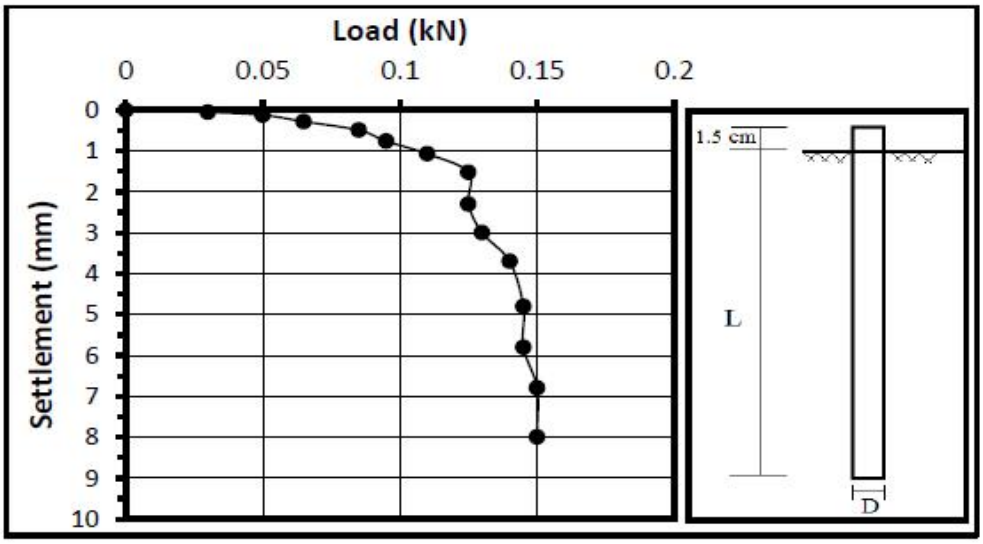

Figure (5): Load-settlement curve of single pile embedded in soil without cavity, L=20 cm, D=1.6 cm.

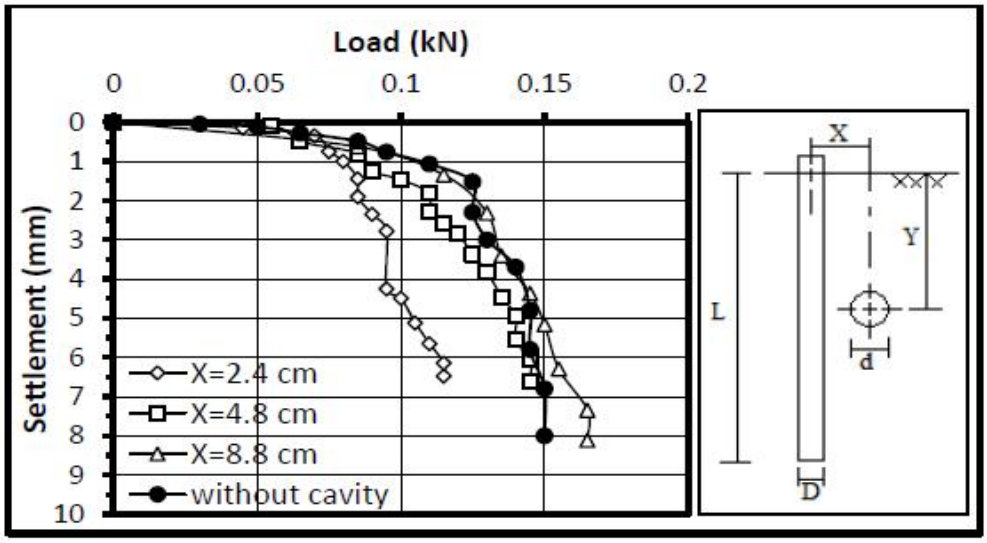

(a) Y/L=0.5

Figure (6) To be Continued.

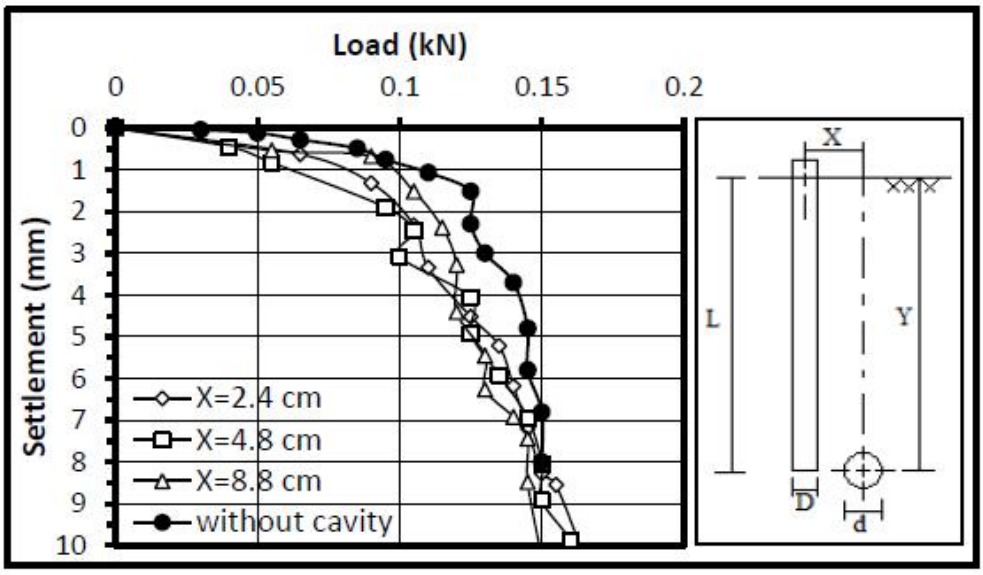

(b) Y/L=1

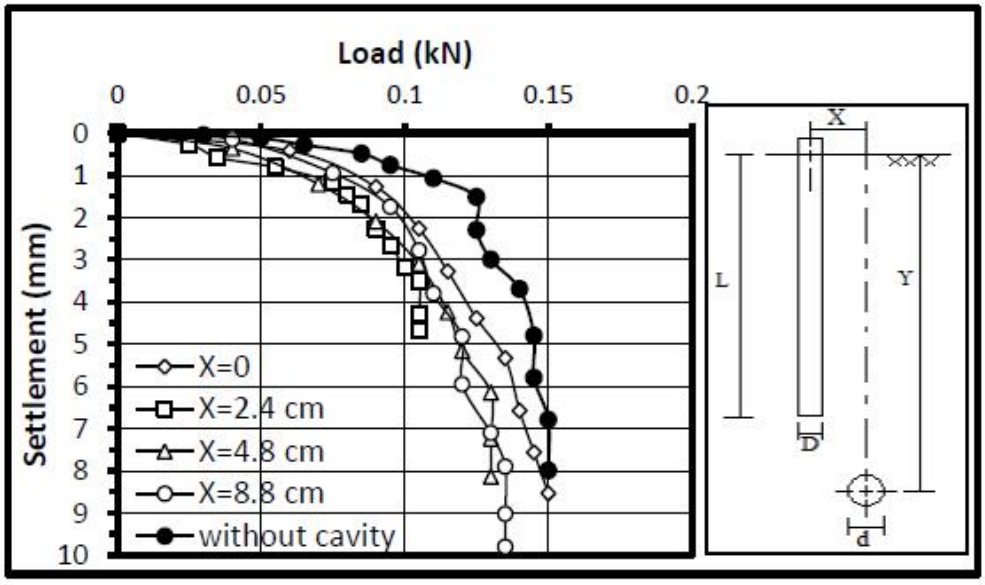

(c) Y/L=1.25

Figure (6): Load-settlement curves of single pile embedded in soil with cavity at different depths, (d/D=1).

The load-settlement curves shown in Figures (5), and (6), indicate that the settlement of pile embedded in soil without cavity is less than the settlement of pile embedded in soil with cavity.

Table (2) shows the values of the failure load obtained from laboratory tests based on strain indicator reading and by using equation (1).

Table (2): Failure load (kN) of single pile embedded in soil with and without cavity obtained from laboratory tests based on strain indicator reading.

With cavity			Without cavity
d/D=1			0.1
Y/L=1.25	Y/L=1	Y/L=0.5	
0.037	-	-	X/D=0
0.09	0.042	0.04	X/D=1.5
0.088	0.07	0.059	X/D=3
0.08	0.08	0.08	X/D=5.5

Figure (7) shows the relationship between the failure load of single pile embedded in soil with cavity and the location of the cavity (X/D) at different depths (Y/L) with (d/D=1).

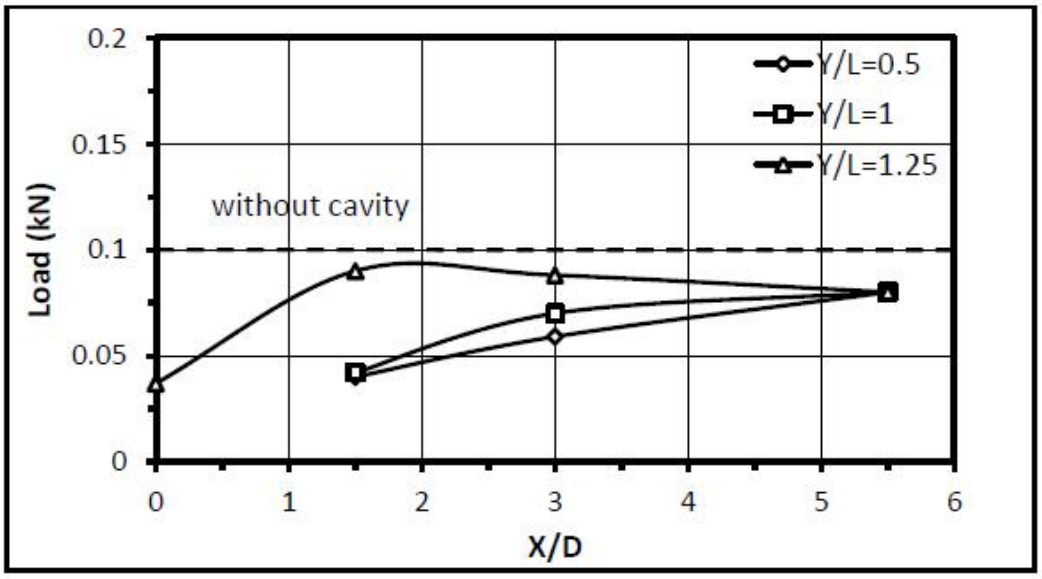

Figure (7): Variation of single pile load versus cavity location of (X/D) at different depths of cavity with (d/D=1).

From Figure (7), it can be seen that the presence of cavity in the soil reduces the ultimate failure load of the pile. The reduction factor in the pile ultimate capacity is defined as:

$$\textbf{Reduction factor} = \frac{\textbf{Load without cavity - Load with cavity}}{\textbf{Load without cavity}} \textbf{ x 100} \quad \text{……..(2)}$$

The reduction factor is about (10% to 60%). As shown in the figure, the load in pile increases with increase of (X/D) due to:

1) Decrease of the zone affected by the presence of cavity.
2) When the cavity is located at a close distance to the pile, it will reduce the soil density and hence decreases the shaft friction along the pile and leads to decrease in the pile failure load.
3) At large distances from the pile; (X/D =5.5), the failure load was found to decrease at (Y/L =1 and 1.25). This may be attributed to the intersection of the failure lines with the cavity which leads to drop of failure load.

The pile load is greatly influenced by the location of the pile tip from the cavity (Y/L) as mentioned by Cheng et al. (2004) who found that the pile axial forces are greatly influenced by the location of pile tip from the tunnel center line. The influence zones are dependent on the location of pile tip, 2D volume loss, soil strength, pile working load, pile size, dilation effect of the granular material, and cavity size. These results are compatible with those obtained by Cheng et al. (2004) and Lee and Bassett (2007).

Group of piles (1x2)

Figure (8) shows the load-settlement curve of group piles (1x2) embedded in soil without cavity. Figure (9) shows the load-settlement curves of group piles (1x2) embedded in soil with cavity of size ratio (d/D=1) at different depths.

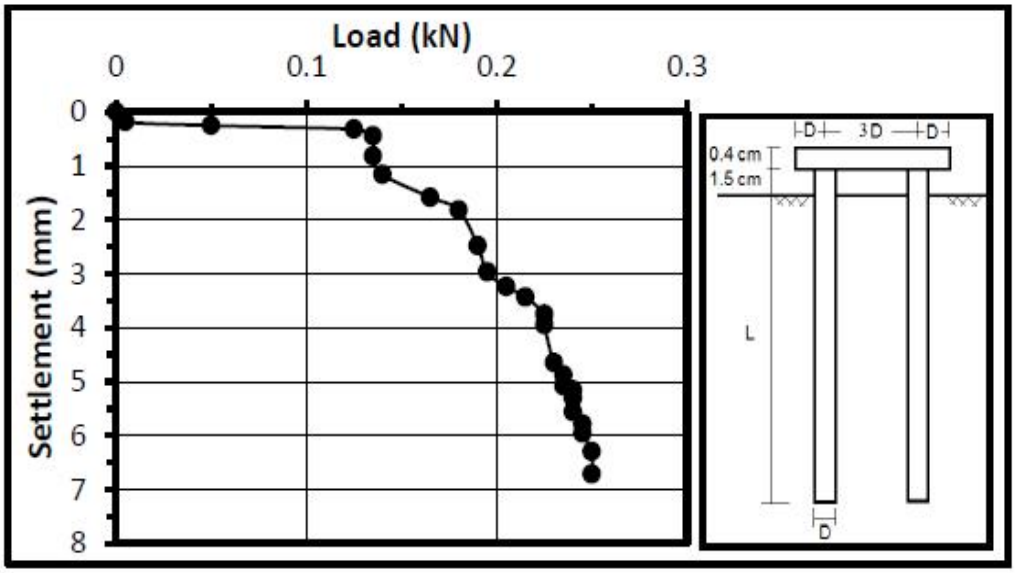

Figure (8): Load-Settlement curve of group piles (1x2) embedded in soil without cavity, L=20 cm, D=1.6 cm.

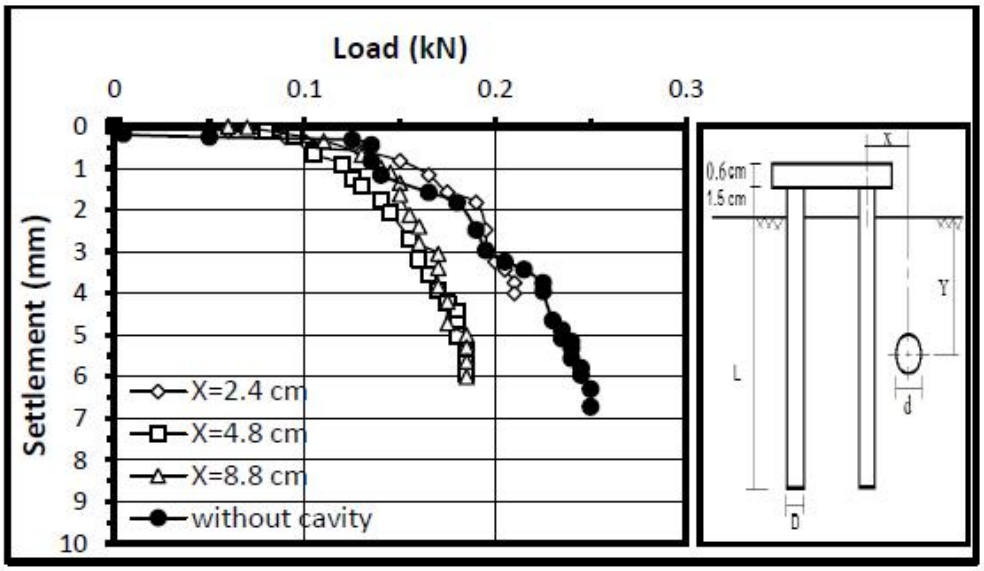

(a) Y/L=0.5

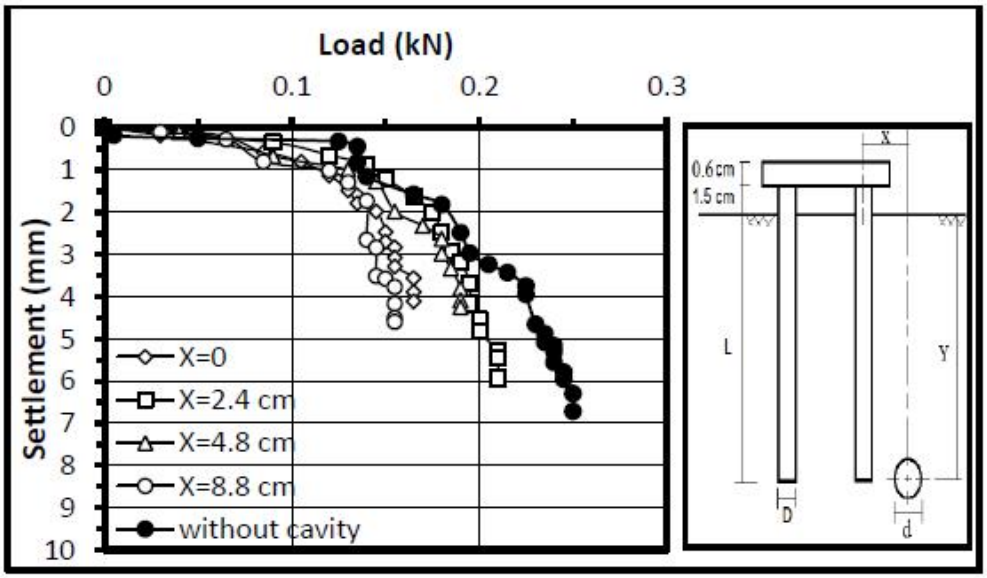

(b) Y/L=1

Figure (9) To be Continued.

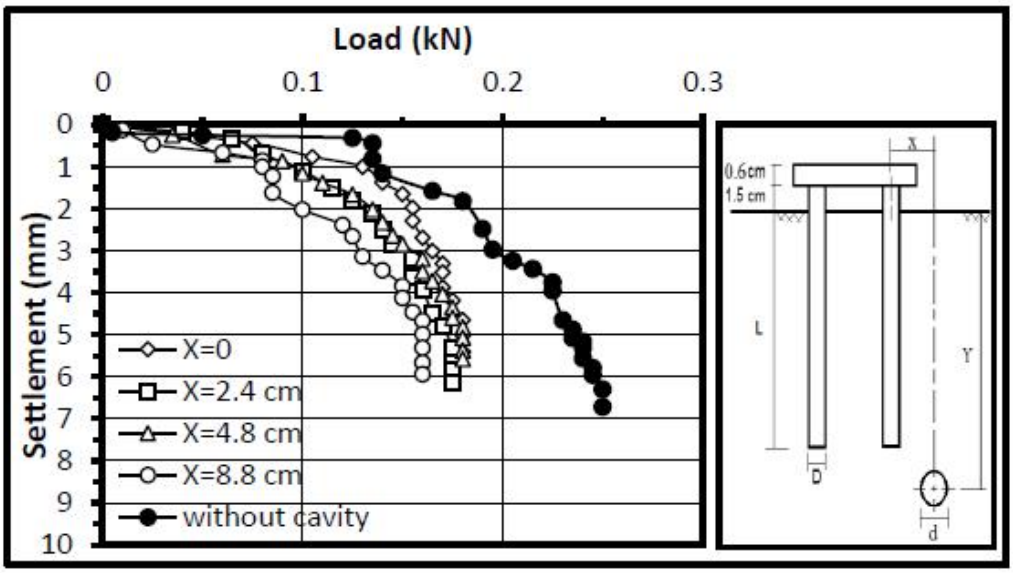

(c) Y/L=1.25

Figures (9): Load-settlement curves of group piles (1x2) embedded in soil with cavity at different depths, (d/D=1).

Table (3) presents the values of the failure load obtained from laboratory tests based on strain indicator reading and using equation (1) for single pile.

The values of failure load illustrated in Table (3) represents the load of group of piles obtained from equation (3), as shown below:

$$Q_{g(u)} = E_g \sum Q_u \qquad \text{…. (3)}$$

where:

$Q_{g(u)}$ = ultimate bearing capacity of group piles,

Q_u = ultimate bearing capacity of each pile without the group effect obtained from equation (1) and based on strain indicator reading , and

E_g = group efficiency from equation (4) (Tomlinson, 2007).

$$E_g = 1 - \frac{\theta(n-1)m + (m-1)n}{90\ m\ n} \qquad \text{. . . . (4)}$$

where :

m = number of columns of piles in a group,

n = number of rows,

$\theta = \tan^{-1}\left(\frac{D}{s}\right)$ in degrees,

D = diameter of pile, and

s = spacing of piles center to center.

The efficiency of pile group (1x2) (Eg) is equal to (0.898).

Figure (10) shows the relationship between the failure load of pile group (1x2) embedded in soil with cavity and the location of the cavity (X/D) at different depths (Y/L) with (d/D=1).

Table (3): Failure load (kN) of group piles (1x2) embedded in soil with and without cavity calculated from the measured strain along the pile.

With cavity			Without cavity
d/D=1			0.16
Y/L=1.25	Y/L=1	Y/L=0.5	
0.085	0.083	-	X/D = 0
0.081	0.03	0.05	X/D =1.5
0.09	0.038	0.06	X/D = 3
0.06	0.052	0.05	X/D = 5.5

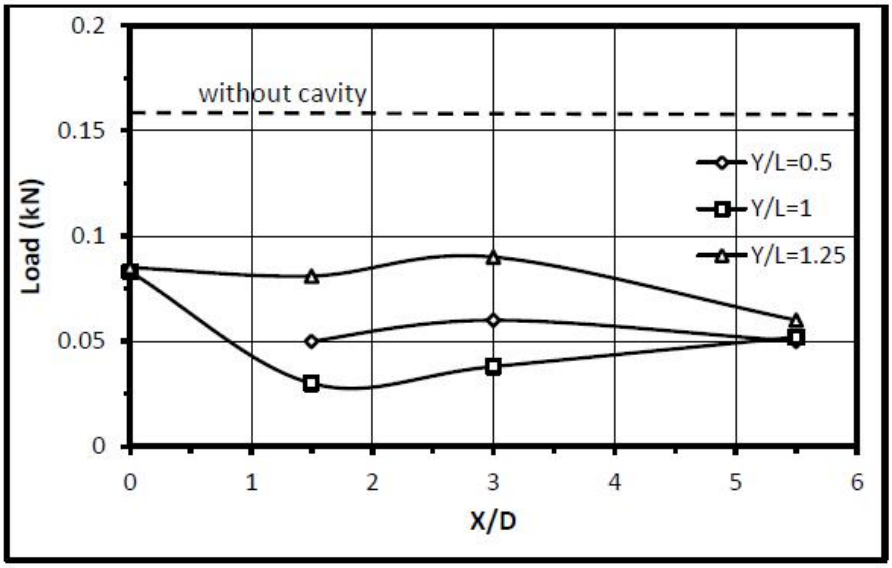

Figure (10): Variation of load of pile group (1x2) versus cavity location of (X/D) at different depths of cavity with (d/D=1).

From Figure (10), it can be seen that the presence of the cavity in the soil reduces the ultimate failure load of the pile. The reduction factor is about (40% to 80%).

CONCLUSIONS

Based on the analysis of the pile model tests, the following conclusions can be raised:

1. The settlement of pile embedded in soil without cavity is less than the settlement of pile embedded in soil with cavity.
2. The load in pile increases with increase of (X/D) due to:
   - Decrease of the zone affected by the presence of cavity.
   - When the cavity is located at a close distance to the pile, it will reduce the soil density and hence decreases the shaft friction along the pile and leads to decrease in the pile failure load.
3. The presence of the cavity in the soil reduces the ultimate failure load of the pile. For single pile, the reduction rate is about (10% to 60%). For pile group (1x2), the reduction rate is about (40% to 80%).
4. As intuitively expected, induced pile axial force is largest for the case where the level of the cavity is located below pile tip because the pile is located within the zone of large displacement.

REFERENCES

[1]Al-Taie, S. M. (2004), "The Performance of Laterally Loaded Piles Embedded in Sandy Soils which Contains Cavities", M.Sc. Thesis, Civil Engineering Department, University of Baghdad. Iraq.

[2]Al-Zayadi, A. A. (2010), "Three Dimensional Analysis of Piled Raft Foundation", PhD. thesis, University of Baghdad, Iraq.

[3]ASTM D 854-2002: "Standard Test Methods for Specific Gravity of Soil Solids by Water Pycnometer", American Society for Testing and Materials.

[4]ASTM D 2487-2000: "Standard Practice for Classification of Soils for Engineering Purposes (Unified Soil Classification System)", American Society for Testing and Materials.

[5] ASTM D 4253-2000: "Standard Test Methods for Maximum Index Density and Unit Weight of Soils Using a Vibratory Table", American Society for Testing and Materials.

[6]ASTM D 4254-2000: "Standard Test Methods for Minimum Index Density and Unit Weight of Soils and Calculation of Relative Density", American Society for Testing and Materials.

[7]ASTM D 3080-1998: "Standard Test Method for Direct Shear Test of Soils under Consolidated Drained Conditions", American Society for Testing and Materials.

[8]Aziz, L. J. (2008): "Lateral Resistance of Single Pile Embedded in Sand with Cavities", Ph.D. Thesis, Building and Construction Engineering Department, University of Technology, Iraq.

[9]Bowels, J.E. (1978), “Engineering Properties of Soils and their Measurement”, Second Edition, McGraw-Hill International Book Company, Tokyo, Japan.

[10] Cheng, C. Y., Dasari, G.R., Leung, C.F., Chow, Y. K., Rosser, H.B. (2004), "3D Numerical Study of Tunnel-Soil-Pile Interaction", Journal of Tunnelling and Underground Space Technology, Vol. 19, issue 4-5, pp. 381-382.

[11] Cheng, C.Y., Dasari, G.R., Chow, Y.K., Leung, C.F. (2007), "Finite Element Analysis of Tunnel-Soil-Pile Interaction Using Displacement Control Model", Tunnelling and Underground Space Technology, 22 (4), pp. 450–466.
[12] Chen, L.T., Poulos, H.G. and Loganathan, N. (1999), "Pile Responses Caused by Tunneling", Journal of Geotechnical and Geoenvironmental Engineering, ASCE, Vol. 125, No. 3, pp. 207-215.
[13] Gordon, T.K., Ng, C.W.W. (2005) "Effects of Advancing Open Face Tunneling on an Existing Loaded Pile", Journal of Geotechncal and Geoenvironmental Engineering, ASCE 131 (2), pp. 193–201.
[14]Kitiyodom, P., Matsumoto, T., Kawaguchi, K. (2005), "A Simplified Analysis Method for Piled Raft Foundations Subjected to Ground Movements Induced by Tunneling", International Journal of Numerical and Analytical Methods in Geomechanics, 29, pp.1485–1507.
[15] Lee, Y. J. and Bassett, R. H. (2007), " Influence Zones for 2D Pile-Soil-Tunneling Interaction Based on Model Test and Numerical Analysis", Tunneling and Underground Space Technology, Vol.22, issue 3, pp. 325-342.
[16] Lee, C.J., Jacobsz, S.W. (2006), "The Influence of Tunneling on Adjacent Piled Foundation", Tunneling and Underground Space Technology, 21 (3–4), 430.
[17] Loganathan, N., Poulos, H.G., Stewart, D.P. (2000), "Centrifuge Model Testing of Tunneling-Induced Ground and Pile Deformations", Géotechnique, 50 (3), pp. 283–294.
[18] Loganathan, N., Poulos, H.G., Xu, K.J. (2001), "Ground and Pile Group Response Due to Tunneling", Soils and Foundations, 41 (1), pp. 57–67.
[19] Morton, J.D., King, K.H. (1979), "Effect of Tunneling on the Bearing Capacity and Settlement of Piled Foundation", Proceedings of Tunneling 79, IMM, London, pp. 57–68.
[20]Mroueh H. and Shahrour, I. (2002), "Three Dimensional Finite Element Analysis of the Interaction between Tunneling and Pile Foundations", International Journal for Numerical and Analytical Methods in Geomechanics, Vol. 26, Issue 3, pp.217-230.
[21]Prakash, S. (1990), "Pile Foundations in Engineering Practice", John Wiley and Sons, New York.
[22]Terzaghi, K. (1943), "Theoretical Soil Mechanics", Wiley, New York.
[23]Tomlinson, M.J (2007)," Pile Design and Construction Practice ", 5th Edition, Taylor and Francis, London and New York.
[24]Xu, K.J., Poulos, H.G. (2001), "3-D Elastic Analysis of Vertical Piles Subjected to ''Passive" Loadings", Computers and Geotechnics, 28, pp.349–375.